

1 **A complex interplay between sphingolipid and sterol metabolism revealed by**
2 **perturbations to the *Leishmania* metabolome caused by miltefosine**

3 Emily G. Armitage^{1,2,3}, Amjed Q. I. Alqaisi^{4,5}, Joanna Godzien¹, Imanol Peña², Alison J. Mbekeani⁴,
4 Vanesa Alonso-Herranz¹, Ángeles López-González¹, Julio Martín², Raquel Gabarro², Paul W.
5 Denny^{4*}, Michael P. Barrett^{3*} and Coral Barbas^{1*}

6
7 1. Centre for Metabolomics and Bioanalysis (CEMBIO), Facultad de Farmacia, Universidad CEU San Pablo,
8 Campus Montepríncipe, Boadilla del Monte, 28668 Madrid, Spain

9
10 2. GSK I+D Diseases of the Developing World (DDW), Parque Tecnológico de Madrid, Calle de Severo Ochoa 2,
11 28760 Tres Cantos, Madrid, Spain

12
13 3. Wellcome Centre for Molecular Parasitology, Institute of Infection, Immunity and Inflammation, College of
14 Medical, Veterinary and Life Sciences & Glasgow Polyomics, University of Glasgow, Glasgow, UK

15
16 4. Department of Biosciences, Durham University, Lower Mountjoy, Stockton Road, Durham, DH1 3LE, UK

17
18 5. University of Baghdad, College of Science, Biology Department, Baghdad, Iraq

19
20 **Running title: Miltefosine on sphingolipids and sterols in *Leishmania***

21 *** Correspondence during publication process to Professor Coral Barbas: cbarbas@ceu.es**

22 *** Correspondence once published to cbarbas@ceu.es, Michael.Barrett@glasgow.ac.uk and**
23 **p.w.denny@durham.ac.uk**

24

25 **ABSTRACT**

26 With the World Health Organization reporting over 30,000 deaths and 200-400,000 new cases
27 annually, visceral *Leishmaniasis* is a serious disease affecting some of the world's poorest people. As
28 drug resistance continues to rise, there is a huge unmet need to improve treatment. Miltefosine
29 remains one of the main treatments for *Leishmaniasis*, yet its mode of action (MoA) is still unknown.
30 Understanding the MoA of this drug and parasite response to treatment could help pave the way for
31 new, more successful treatments for *Leishmaniasis*. A novel method has been devised to study the
32 metabolome and lipidome of *Leishmania donovani* axenic amastigotes treated with miltefosine.
33 Miltefosine caused a dramatic decrease in many membrane phospholipids (PLs), in addition to
34 amino acid pools, while sphingolipids (SLs) and sterols increased. *Leishmania major* promastigotes
35 devoid of SL biosynthesis through loss of the serine palmitoyl transferase gene (Δ LCB2) were 3-fold
36 less sensitive to miltefosine than WT parasites. Changes in the metabolome and lipidome of
37 miltefosine treated *L. major* mirrored those of *L. donovani*. A lack of SLs in the Δ LCB2 was matched
38 by substantial alterations in sterol content. Together these data indicate that SLs and ergosterol are
39 important for miltefosine sensitivity and perhaps, MoA.

40

41 **INTRODUCTION**

42 Infectious diseases continue to cause great morbidity and mortality worldwide(1). New drugs are
43 required and will need to be continuously replenished as resistance to antimicrobials increases.
44 Understanding the mode of action (MoA) of currently available treatments against microbial
45 diseases offers a means to highlight targets for new treatments. Metabolomics plays an important
46 role in this discovery and development of new medicines for infectious diseases(1).

47 The *Leishmaniases* are a spectrum of neglected tropical diseases caused by protozoa of the genus
48 *Leishmania*. Individual species provoke different clinical manifestations including visceral
49 *Leishmaniasis* caused by *Leishmania donovani* and *Leishmania infantum*(2) which is fatal if not
50 treated. Existing therapeutic options are limited(3), so the search for alternative therapies continues.
51 Two key developmental stages of *Leishmania*: amastigotes and more commonly promastigotes are
52 used for *in vitro* studies of drug MoA. Promastigotes are the form found in the sand fly vector, while
53 amastigotes exist in the mammalian host. Development of axenic cultures, having physiological
54 similarity to the macrophage resident forms in mammalian infections, has made it possible to study
55 amastigotes *in vitro*(2).

56 Metabolomics seeks comprehensive measurements of small molecules in a given system. However,
57 the dynamic range in abundance and broad physicochemical diversity of metabolites is such that a
58 single analytical platform is lacking. Here, a combined liquid chromatography – mass spectrometry
59 (LC-MS) and capillary electrophoresis – mass spectrometry (CE-MS) approach was used to increase
60 coverage of the *Leishmania* metabolome and applied to study MoA of miltefosine, the first drug
61 approved for oral treatment of *Leishmaniasis*. Metabolomics has proven useful in drug MoA studies
62 for *Leishmania* promastigotes(4–13), but so far not for *L. donovani* amastigotes. *L. mexicana*
63 amastigotes were recently studied using metabolomics to show that amastigote differentiation is
64 associated with the induction of a distinct stringent metabolic state(14), in both lesion-derived and
65 *in vitro* differentiated amastigotes.

66 Several suggestions have been made regarding the anti-leishmanial action of miltefosine: induction
67 of apoptosis-like death(15, 16), or disruption of metabolite transport(4, 17, 18). The uptake of
68 miltefosine in *Leishmania* is dependent on transmembrane lipid transporters, most notably the
69 flippase LdMT and its accessory protein – LdRos that are commonly lost with selection of
70 resistance(19). More recently, using cosmid-based functional cloning coupled to next-generation

71 sequencing, genes involved in ergosterol biosynthesis and phospholipid (PL) translocation were
72 suggested to contribute to resistance in *L. infantum*(20).

73 Metabolomic analyses of miltefosine treated *L. infantum* showed a general depletion of intracellular
74 metabolites(6) and similar studies in other *Leishmania* demonstrated lipid remodelling(21–24).
75 Biochemical modifications to different lipid classes have been reported in the membranes of
76 miltefosine treated *L. donovani* promastigotes(22). In addition to diminishing phosphatidylcholine
77 (PC), miltefosine was found to double sterol composition too(22). Effects of miltefosine treatment
78 on lipid metabolism in promastigotes of *L. infantum*(6) have also been observed using
79 metabolomics, although only lipid class rather than individual lipid species were resolved. Combining
80 CE-MS to analyse polar and ionic metabolites and reversed phase LC-MS to reveal specific lipidomic
81 changes in *L. donovani* has allowed a more detailed analysis into the MoA in axenic amastigotes
82 presented herein.

83 Substantial changes in sphingolipid (SL) and sterol metabolism were revealed in miltefosine treated
84 *L. donovani* promastigotes. SLs were first reported in *L. donovani* more than 20 years ago(25) and
85 along with sterols, have since received attention in many species(26–28). *Leishmania* obtain SLs via
86 salvage or *de novo* synthesis(29), and they play important roles in differentiation, replication,
87 trafficking and virulence(29). The prominent, and most studied, SL identified is inositol
88 phosphoceramide (IPC), although *Leishmania* are believed to exhibit a complete and functional SL
89 pathway involving both biosynthesis and degradation(28, 30). A more comprehensive analysis of
90 different SLs may identify other key targets of SL metabolism for therapy. To study the viability of
91 *Leishmania* without SL synthesis, a mutant was created by deletion of the gene encoding the
92 essential catalytic subunit of the serine palmitoyltransferase (Δ LCB2), the first and rate-limiting step
93 in SL biosynthesis(28, 31). Surprisingly, this mutant was viable, indicating a dispensable role for SLs in
94 *Leishmania*, unlike in the related parasite *Trypanosoma brucei*(32). It was suggested that the sterol
95 composition of the *Leishmania* plasma membrane, where ergosterol replaces cholesterol as the

96 primary membrane sterol, could enable this(32). Here perturbations to *Leishmania* SL and sterol
97 metabolism on miltefosine treatment are described, the interplay between these metabolite
98 families is considered and the role sterols play in drug sensitivity proposed.

99 **RESULTS AND DISCUSSION**

100 In order to define the optimal protocol for sampling/quenching/extracting/analysing metabolites
101 from *L. donovani* axenic amastigotes, a method was developed as described below and further in the
102 Supplementary Information (SI - file 1). The extraction procedure was optimised such that LC-MS and
103 CE-MS analyses could be performed from single samples of as few as 1×10^7 parasites (SI Figure 1S:).
104 For *L. donovani*, samples were treated with 4.47 μM (the observed EC_{50} at 72 hours, consistent with
105 the literature (33)) or 13.41 μM (three times the observed EC_{50} at 72 hours) miltefosine and
106 harvested after 5h or 24h of exposure to observe the initial effects of the drug. For *L. major*, samples
107 were treated with 10 μM or 30 μM miltefosine and harvested after 5h of exposure. DMSO controls
108 were prepared alongside treated samples at each time-point for both species. Results from method
109 development stages are detailed in the SI, where a comparison of methanol extraction and a more
110 comprehensive extraction for lipidomics using LC-MS is shown in figure 2S, profiles obtained using
111 LC-MS and CE-MS analysis of different extractions are shown in figure 3S and the final optimised
112 dual extraction procedure to obtain different extracts for LC-MS and CE-MS analysis from single
113 samples is shown in figure 4S.

114 Metabolomic determination of *Leishmania* response to miltefosine

115 With the exception of the aforementioned work on *L. mexicana* amastigotes(14), the few studies on
116 drug MoA in *Leishmania* have focussed on the promastigote form(2–10). The aim of this research
117 was to explore effects on metabolism of miltefosine in *L. donovani* axenic amastigotes and, as a
118 result of these findings, in *L. major* promastigotes.

119 After verification of quality (SI Figure 5S), data were divided into separate sets and differences
120 between treated and untreated parasites identified. Around 20 metabolites, including the drug
121 itself, were detected only in treated samples. These features, listed after the supplementary tables
122 in supplementary information, were all found to elute with the drug and therefore most likely
123 enhanced by the ionisation of the drug. These could not be identified as endogenous lipids and were
124 therefore assumed to be mass spectrometry derivatives of the drug itself. All were removed prior to
125 multivariate analysis to avoid separation based on presence or absence of drug alone. Identification
126 was performed for metabolite features found to increase/decrease with treatment after 5 or 24 h of
127 exposure, determined by a p -value <0.05 (Student's two-tailed t -test, $n=6$ per group) and a fold
128 change of ± 1.5 , calculated for at least one of the comparisons made. Identification of metabolites
129 found by CE-MS was confirmed by injection of authentic standards (as detailed in Supplementary
130 Table 1). Lipids detected using LC-MS were annotated considering chemical properties and elution
131 order. Miltefosine treatment affected different metabolic classes and possible impact on MoA is
132 discussed below, based on data presented in the Supplementary Tables (STs), a description for which
133 is given in SI.

134 *L. donovani* axenic amastigotes

135 Miltefosine has been proposed to affect the transport of different metabolites(4, 17, 18). Consistent
136 with previous literature(6), miltefosine induced decreases in the majority of internal metabolites
137 detected by CE-MS, as shown in Table 1, which could be associated with impaired uptake. Figure 1
138 shows the abundances of metabolites associated with arginine metabolism detected in this study.
139 Arginine is a precursor to polyamine biosynthesis and a protein building block. Its intracellular
140 concentration is controlled by dedicated sensory protein transporters(10, 18), which have been
141 suggested as targets of miltefosine(4). Arginase, which catalyses the hydrolysis of arginine to
142 ornithine, also contribute to the intracellular concentration of arginine. The co-ordinated decrease in
143 arginine and ornithine may indicate a reduction in precursor levels (through blocking arginine

144 transport), a notion consistent with previously reported literature (34, 35). Another metabolite that
145 shares the same mass but has a distinct migration time to citrulline was identified as argininic acid
146 which is considered an endpoint of arginine metabolism previously found in different *Leishmania*
147 species, including *L. donovani*(36). Its concentration was substantially reduced with treatment at
148 both time-points and doses (up to 3-fold) in this research.

149 While data from CE-MS largely confirmed observations in the literature, the approach here has given
150 a finer-grained view of the effect of miltefosine on lipids. Compared to mammals, *Leishmania*
151 membrane lipids differ substantially in composition and function, making them important for
152 viability and virulence as well as potential drug targets(29). Lipids have been analysed previously in *L.*
153 *donovani*(7, 22, 29, 37), as have changes in lipid metabolism connected to miltefosine treatment(21–
154 23, 38, 39). Here we demonstrate more detail on individual lipid species than has previously been
155 reported.

156 In *L. infantum*, miltefosine was reported to alter 10 % of the metabolome, purportedly due to
157 compromised outer membrane integrity leading to lysis(6). Here, a general decrease in membrane
158 PL abundance was observed in *L.donovani* axenic amastigotes (see STs 2, 3 and 4 for specific lipids).
159 Miltefosine was reported by Zufferey *et al.* (2002) to inhibit PC biosynthesis, diminishing levels in *L.*
160 *donovani* promastigotes leading to growth arrest(21). Phospholipase D activity was unaffected by
161 the drug, hence inhibition of the choline transporter was proposed to underlie the reduction in PC
162 biosynthesis(21) . A number of PCs and other PLs were found diminished in this study too (ST2).

163 Other considerable effects of treatment observed were increases in sterols and, to an even greater
164 extent, SLs. To investigate this further, all filtered LC-MS data were scanned to identify peaks
165 identifiable as SLs (even if the relative levels in treated and untreated parasites were not statistically
166 different). Figure 2 shows the trends observed in SLs, where data are plotted for un-treated
167 parasites and parasites treated with the lowest dose of miltefosine at 24 h. A dramatic and

168 significant (5-fold) increase in sphingosine abundance induced by miltefosine ($p=2\times 10^{-6}$) was
169 mirrored by a 3-fold increase in sphinganine ($p=7\times 10^{-4}$). All detected ceramides were also
170 substantially increased by 24 h, as shown and detailed in Supplementary Table 3.

171 *L. major* promastigotes

172 *Leishmania* SL metabolism has been best studied in the promastigote form of *L. major*, where a
173 Δ LCB2 mutant lacking the first enzyme of the biosynthetic pathway, serine palmitoyl transferase, is
174 available(28, 31). The effects of miltefosine in these *L. major* promastigotes were therefore
175 investigated. The efficacy of miltefosine was established against both the Δ LCB2 mutant and wild
176 type lines; the EC_{50} for the wild type was 6.83 μ M, consistent with previous literature (33), whilst for
177 mutant was three times higher at 21.21 μ M. The lipidome of these parasites revealed major
178 differences between the wild type and Δ LCB2 lines and the effect of miltefosine was also compared.
179 Lipids identified with marked differences in abundance between any experimental groups compared
180 are detailed in STs 5, 6 and 7. As in *L. donovani*, miltefosine itself and around 20 other features were
181 detected only in treated samples. Miltefosine was identified in both wild type and Δ LCB2 mutant,
182 with no significant difference in relative concentration ($p=0.09$ for the lower dose and $p=0.45$ at the
183 higher dose). This demonstrated that the 3-fold resistance of the mutant was not due to inhibited
184 import. As in *L. donovani* in this study and reported in *L. infantum* previously(6), miltefosine caused
185 substantial effects in levels of numerous PLs in *L. major* too. This reduction may be due to reduced
186 import of PLs or choline, or reduced *de novo* biosynthesis.

187 Miltefosine's effects on *L. major* SLs were similar to those observed after 24h of exposure in *L.*
188 *donovani* amastigotes. Figure 3 shows the fold changes for both doses. As can be seen, some SLs
189 were detected only in *L. donovani* or only in *L. major*. This may be due to species specific differences
190 and could even be due to differences in the mechanism of each species given that they cause
191 different forms of leishmaniasis (*L. donovani* causing the visceral form and *L. major* the cutaneous

192 form). The *L. major* Δ LCB2 mutants lack most SLs, in accordance with them being devoid of SL
193 biosynthesis. Sphingosine and ceramide (d36:1) were, however, detected indicating that they are
194 acquired from the media. Likewise, SM may also be derived from the media since there is no
195 evidence that *Leishmania* synthesize SM, although they do possess SMase which has been shown to
196 be essential in degrading host-derived SM to promote parasite survival, proliferation and
197 virulence(40). The increase in SLs could indicate a stimulatory effect of miltefosine on biosynthesis or
198 inhibition of a catabolic pathway, the latter seeming more likely since the mutant also accumulates
199 higher levels of the two SLs detected (SM and ceramide d36:1 upon treatment (Figure 3).

200 As in *L. donovani*, sterols were also increased by treatment in *L. major* wild type, though not in
201 Δ LCB2 mutants. The identification of sterols poses a particular challenge since many in the pathway
202 share identical masses. However, using the calculated LogP values it was possible to identify each
203 based on their elution order in the LC-MS data, as shown in SI file 2. Figure 4 shows the ergosterol
204 biosynthesis pathway and highlights observed increases in *L. donovani* after 5 h (blue arrows), 24 h
205 (red arrows) and in *L. major* wild type after 5 h (green arrows) of miltefosine exposure. Trends were
206 the same for both concentrations of the drug, except for fecosterol at the higher dose in *L. donovani*
207 which was increased albeit not significantly.

208 Although sterol differences were not observed with treatment in Δ LCB2 mutants (ST 7), comparison
209 to the un-treated wild type revealed dramatic differences in sterol metabolism, particularly with
210 respect to ergosterol and cholesterol. This alteration in sterol composition in the selection of the
211 mutant is particularly noteworthy since it enables the mutant to survive without SL synthesis, while
212 the change in sterol composition may stabilise membranes in the face of miltefosine treatment,
213 emphasising the complex interplay between SL and sterol metabolism. As shown in the
214 chromatographic peaks in Figure 4, ergosterol levels were significantly reduced (approximately
215 halved $p=5 \times 10^{-14}$) in the Δ LCB2 relative to wild type whilst cholesterol levels were around 3-fold
216 more abundant $p=8 \times 10^{-12}$. Cholesterol is probably scavenged in *Leishmania*(26). Ergosterol was

217 significantly increased with treatment in the wild type and of much lower abundance in the mutant
218 which exhibit a 3-fold reduced sensitivity to the drug. 5,7,22,24(28)-Ergostatetraenol, which
219 precedes ergosterol in its synthetic pathway, is also dramatically more abundant in Δ LCB2 mutants
220 compared to wild type, which suggests that the final step in ergosterol synthesis (catalysed by erg4)
221 is diminished in the mutant. Two further sterols, which share the same mass as ergosterol,
222 5,7,24(28)-Ergostatrienol and 5-dehydroepisterol, were observed in the mutant but were below the
223 limit of detection in the wild type. Their accumulation may also occur due to the reduced production
224 in ergosterol biosynthesis later in the pathway.

225 Δ LCB2 *Leishmania* mutants are viable while the same enzyme is essential to African trypanosomes.
226 This has been proposed to be due to *Leishmania* depending on ergosterol as its primary sterol
227 rather than cholesterol as in *T. brucei*(29). However, since the Δ LCB2 mutant exhibits much higher
228 cholesterol and lower ergosterol concentrations relative to wild type, the simplistic view of changes
229 in cholesterol versus ergosterol appears to be inadequate to explain the essential nature of SL
230 synthesis in *T. brucei*. Though the magnitude of this sterol balance is not as severe as in *T. brucei*,
231 retained viability in the absence of SL synthesis is likely to be due to other reasons. As observed in
232 the *L.major* Δ LCB2 mutants, ergosterol reduction has been reported in a strain of *L. infantum*
233 resistant to 200 μ M miltefosine compared to wild type(41), although the mechanism of resistance
234 was reported to be associated to mutations in the miltefosine transporter. In *L.donovani*
235 promastigotes, membrane sterol depletion has been correlated with reduced sensitivity to
236 miltefosine(42). In that study the authors tested a hypothesis that lipid rafts could be involved in
237 miltefosine action by destabilising these micro-domains through depletion of sterols using either
238 methyl- β -cyclodextrin (MCD) or cholesterol oxidase (CH-OX). Sterol depletion showed no significant
239 effects on the viability of either wild type or mutant, however MCD treatment significantly
240 decreased the susceptibility of wildtype to miltefosine (around 2-fold) although CH-OX depletion
241 caused no significant effect. Since MCD has less specificity in sterol extraction than CH-OX, MCD is

242 likely to deplete ergosterol and other sterols in addition to cholesterol, pointing to a possible link
243 between ergosterol depletion and reduced miltefosine activity. Increases in ergosterol in *L. donovani*
244 and *L. major* (wild type) co-ordinated with an increase in SLs reported here may also point towards a
245 function of lipid micro-domain complexes of sterols and SLs(27, 29, 42) in miltefosine's effects on
246 the parasites. Apoptosis has been proposed as an effect of miltefosine in tumour cells relating to
247 lipid micro-domains(43–45). Though the existence of apoptosis in *Leishmania* has been
248 challenged(46), various indications point to miltefosine inducing an apoptosis-like death in
249 *L. donovani* promastigotes(16). It is clear that miltefosine treatment causes profound changes to the
250 lipid content of *Leishmania* amastigotes and promastigotes and that alteration in lipid composition
251 such as a loss of SL biosynthesis and an accompanying change in sterol metabolism, impact on this
252 action of the drug.

253 CONCLUSION

254 A robust platform offering broad coverage of *Leishmania* metabolites using two complementary
255 techniques was developed to study miltefosine MoA. In addition to revealing miltefosine's effects
256 on internal metabolites and possible interference with membrane transport, many lipid species were
257 shown to be perturbed by treatment and importantly SLs and sterols were found to increase. These
258 findings, initially observed in *L. donovani* axenic amastigotes, were confirmed in *L. major*
259 promastigotes for which a defined Δ LCB2 mutant, devoid of SL biosynthesis was available. These
260 mutant parasites lacked SLs, other than those derived from the culture medium, and sterol
261 metabolism was drastically altered compared with wild type. This lipidomic remodelling was
262 associated with a 3-fold reduction in sensitivity to miltefosine. Coupled with the observation that
263 sterol concentrations increase when both *L. major* and *L. donovani* wild type parasites were exposed
264 to miltefosine, a major role for these lipids in miltefosine resistance and, perhaps, MoA is indicated.

265 MATERIALS AND METHODS

266 Experimental design

267 In order to define the optimal protocol for sampling/quenching/extracting/analysing metabolites
268 from *L. donovani* axenic amastigotes, a two-stage experiment was designed that i) allowed a
269 reproducible global profile of metabolites to be obtained and ii) allowed the execution of the
270 optimised protocol in the exploration of miltefosine MoA. It was necessary to optimise parasite
271 seeding densities and harvesting numbers to work with 5 h and 24 h time-points to obtain sufficient
272 biomass for metabolomics analyses, while also ensuring log phase of growth (metabolic steady state)
273 in parasites at the time of harvesting. Parasites were always seeded from log phase cultures to
274 minimise lag phase (particularly important at 5 h). Optimal seeding densities were determined as
275 6.67×10^6 parasites/mL for samples to be harvested at 5h and 1.33×10^6 parasites/mL for samples to
276 be harvested at 24h. Details of the method development are given in full in SI.

277 Chemicals and reagents

278 The axenic culture medium used in all experiments was prepared from one batch prepared 'in-
279 house' as described in Peña I. *et al.*(2). The culture medium used for *L. major* wild type and was
280 Schneider's *Drosophila* media (Sigma Aldrich) supplemented with heat inactivated foetal bovine sera
281 (15%). All methanol used was HPLC-grade and formic acid was analytical grade. These chemicals in
282 addition to formaldehyde solution and PBS were purchased from Sigma-Aldrich. Ultrapure water
283 was obtained using a Milli-Qplus 185 system (Millipore, Bilerica, MA, USA).

284 Sample collection and quenching of metabolism

285 *L. donovani* strain 1S2D (WHO designation: MHOM/SD/62/1S-CL2D)(47) was cultured by cycling
286 between promastigotes and axenic amastigotes using protocols from prior work(2). Briefly, the
287 promastigote form was grown at 29 °C and amastigote forms were grown at 37 °C with 5 % CO₂ in
288 different media adapted from De Rycker, *et al.*(48). For experiments with miltefosine, three T75

289 flasks were prepared (with 30 mL culture at the appropriate densities for 5h or 24 h as described
290 above) for each condition: non-treated parasites, parasites treated with the lower dose of
291 miltefosine (4.47 μM) and parasites treated with the higher dose of miltefosine (13.41 μM).

292 At the time of sample harvesting, culture from each flask was divided equally into two 15 mL Falcon
293 tubes resulting in six replicate samples for each condition. Before the division, 50 μL of each culture
294 was collected into Eppendorf tubes to which 50 μL formaldehyde was added and samples were
295 stored at 4 $^{\circ}\text{C}$ to be counted later in order to record the exact number of parasites from each flask at
296 the time of harvesting. At the time of harvesting and throughout the subsequent processes, samples
297 were maintained at 4 $^{\circ}\text{C}$.

298 After collection of culture, each sample was centrifuged at $1500 \times g$ at 4 $^{\circ}\text{C}$ for 15 min after which
299 medium was decanted and parasites were washed in 2 mL PBS (maintained at 4 $^{\circ}\text{C}$), then samples
300 were transferred to 2 mL Eppendorfs. From each sample, 10 μL was taken and fixed with 10 μL of
301 formaldehyde and stored at 4 $^{\circ}\text{C}$ to be counted later in order to record the exact number of
302 parasites in each sample immediately before quenching. Samples were subsequently centrifuged at
303 $1500 \times g$ at 4 $^{\circ}\text{C}$ for 15 min, PBS was decanted and 200 μL ice cold methanol was added to each
304 sample that were immediately stored at -80°C until extraction and metabolomics analysis. Figure 15
305 of Supplementary Information shows the workflow for the developed method for sampling.

306 *Leishmania major* parasites (MHOM/IL/81/Friedlin; FV1 strain) and a mutant in which the catalytic
307 subunit of serine palmitoyltransferase had been deleted by homologous recombination (ΔLCB2)(31)
308 were cultured as log phase promastigotes at 26°C . Samples were prepared for metabolomics as
309 described for *L. donovani* with the appropriate miltefosine doses as described above, except 10 μM
310 or 30 μM were used for the lower and higher dose of miltefosine respectively.

311 Metabolite extraction

312 Extraction blanks were prepared following all stages of extraction. On the day of analyses,
313 metabolites were extracted and supernatants analysed by LC-MS (and for all *L. donovani* samples in
314 CE-MS too). Samples were prepared by first evaporating extracts to dryness using a speed vacuum
315 concentrator (Eppendorf, Hamburg, Germany), after which 200 mg of 425-600 μm acid-washed glass
316 beads were added. Then to *L. donovani* samples, 575 μL of 100 % methanol were added, before
317 which samples were vortex mixed for 10 min and placed in a tissue lyzer for 30 min at 50 Hz. Finally
318 samples were centrifuged at $16,000 \times g$ at 4°C for 10 min and 80 μL of the resulting supernatants
319 were collected into LC-MS vials to be analysed directly. To the remaining samples (for CE-MS),
320 165 μL water were added and all vortex mixed for 30 min then centrifuged at $16,000 \times g$ at 4°C for
321 10 min, before being evaporated to dryness and re-suspended in 100 μL of water containing 0.2M
322 methionine sulfone (internal standard) and 0.1mM formic acid was added to each. QC samples for
323 LC-MS and CE-MS were prepared by collecting 10 μL from each sample into a single pool. For *L.*
324 *major*, only LC-MS extracts were prepared and therefore after evaporation, 120 mg of 425-600 μm
325 acid-washed glass beads and 350 μL methanol were added for extraction and 270 μL of the resulting
326 supernatants following extraction were collected into LC-MS vials to be analysed directly, from
327 which 30 μL was subtracted from each into a pool.

328 Analysis of extracts by LC-MS and CE-MS

329 For each analysis, extraction blanks were injected at the start of the analysis followed by eight
330 injections of the QC sample in order to ensure system stability, before the injection of samples
331 analysed in a random order with the QC injected after every sixth sample until the end of the
332 analysis. All instrumentation was from Agilent Technologies. For LC-MS, a 1290 infinity LC equipped
333 with reverse-phase column (Zorbax Extend C_{18} 50 \times 2.1 mm, 3 μm ; Agilent) was coupled to a 6550 Q-
334 TOF MS with electrospray ionisation source and operated in both positive and negative mode. For
335 CE-MS the instrument consisted of a 7100 CE coupled to a 6224 TOF MS operated in positive mode.
336 Details of the analytical procedures based on previously published methods(49, 50) are given in SI.

337 Data analysis and feature identification

338 Data from both platforms were processed using recursive analysis in Mass Hunter Profinder
339 (B.06.00, Agilent) software as detailed in SI. Data were reprocessed considering ions such as [M+H]⁺
340 and [M+Na]⁺, neutral water loss and the maximum permitted charge state was double. Alignment
341 was performed based on *m/z* and RT similarities within the samples. Parameters applied were 1 %
342 for the RT window and 20 ppm for mass tolerance.

343 Data treatment consisted of filtering based on quality, following the same procedure for each
344 dataset (*L. donovani*: LC-MS positive ion mode, LC-MS negative ion mode, CE-MS positive ion mode;
345 *L. major*: LC-MS positive ion mode, LC-MS negative ion mode). Data were filtered based on quality
346 using a quality assurance procedure described previously (QA+)(51). This involved retaining features
347 present in QCs at a rate of 80 % or absent in QCs (defined as presence < 20 %). For features present
348 in QC samples, only those with RSDs < 30 % were kept and for those absent, RSD was not calculated.
349 Then, for each comparison separately (5h, or 24h, wild type or Δ LCB2 mutant), features were further
350 filtered to keep only those present in at least five out of six of the replicates from one of the groups
351 simultaneously compared (resulting in a slightly different, but relevant dataset for each comparison).

352 For *L. donovani* multivariate analysis was employed firstly to observe the stability in each analysis
353 (LC-MS in positive and negative ionisation modes or CE-MS) as a whole and then for each time point
354 separately to investigate the effect of the drug on the parasite metabolome. To probe specific
355 questions on the effect of miltefosine at different time points or doses, fold-changes and *p*-values
356 were calculated in order to assess the degree of significance of any difference observed in the raw
357 data.

358 All significantly different metabolite features between un-treated and treated parasites at any dose,
359 determined by determined by a *p*-value <0.05 (Student's two-tailed *t*-test, *n*=6 per group) and a fold
360 change, \pm 1.5 were identified. Identification was performed searching *m/z* against Metlin

361 (<http://metlin.scripps.edu>) and lipidMAPS (<http://lipidMAPS.org>), considering the same adducts as
362 those described for data re-processing. Annotations were assigned to *m/z* values for metabolite
363 features considering i) mass accuracy (maximum mass error 10ppm); ii) isotopic pattern distribution;
364 iii) possibility of cation and anion formation and iv) adducts formation. This method of enhanced
365 annotation was based on our previously published work(49). Where possible, identifications were
366 compared by retention time order to standards analysed in-house. For CE-MS, definitive
367 identifications were made for a number of metabolites through analysis of authentic standards
368 analysed under the same conditions as the experiment, whereby samples were analysed again
369 followed by the same samples spiked with authentic standards to prove the identity.

370 All data analysed during this study are included in this published article and in the supplementary
371 tables (Supplementary Information files).

372 **ACKNOWLEDGEMENTS**

373 Authors acknowledge funding provided by the Tres Cantos Open Lab Foundation (TCOLF: program code
374 TC132). In addition, authors at Universidad San Pablo CEU acknowledge Spanish Ministerio de Economía y
375 Competitividad (CTQ2014-55279-R), MPB is funded by a core grant to the Wellcome Centre for Molecular
376 Parasitology (104111/Z/14/Z) and authors at Durham University acknowledge funding from the BBSRC
377 (BB/M024156/1) and MRC (MR/P027989/1) in addition the Government of Iraq.

378 **REFERENCES**

- 379 1. Kim D-H, Creek DJ. 2015. What role can metabolomics play in the discovery and development
380 of new medicines for infectious diseases? *Bioanalysis* 7:629–631.
- 381 2. Peña I, Pilar Manzano M, Cantizani J, Kessler A, Alonso-Padilla J, Bardera AI, Alvarez E,
382 Colmenarejo G, Cotillo I, Roquero I, de Dios-Anton F, Barroso V, Rodriguez A, Gray DW,
383 Navarro M, Kumar V, Sherstnev A, Drewry DH, Brown JR, Fiandor JM, Julio Martin J. 2015.
384 New compound sets identified from high throughput phenotypic screening against three

- 385 kinetoplastid parasites: an open resource. *Sci Rep* 5:8771.
- 386 3. Pedrique B, Strub-wourgaft N, Some C, Olliaro P, Trouiller P, Ford N, Pécoul B, Bradol J. 2013.
387 The drug and vaccine landscape for neglected diseases (2000 – 11): a systematic
388 assessment. *Lancet Glob Heal* 1:371–379.
- 389 4. Canuto GAB, Castilho-martins EA. 2014. Multi-analytical platform metabolomic approach to
390 study miltefosine mechanism of action and resistance in *Leishmania*. *Anal Bioanal Chem*
391 406:3459–3476.
- 392 5. Saunders EC, Ng WW, Chambers JM, Ng M, Naderer T, Kro JO, Likic VA, Mcconville MJ. 2011.
393 Isotopomer Profiling of *Leishmania mexicana* Promastigotes Reveals Important Roles for
394 Succinate Fermentation and Aspartate Uptake in Tricarboxylic Acid Cycle (TCA) Anaplerosis ,
395 Glutamate Synthesis , and Growth. *J Biol Chem* 286:27706–27717.
- 396 6. Vincent IM, Weidt S, Rivas L, Burgess K, Smith TK, Ouellette M. 2014. Untargeted
397 metabolomic analysis of miltefosine action in *Leishmania infantum* reveals changes to the
398 internal lipid metabolism. *Int J Parasitol Drugs Drug Resist* 4:20–27.
- 399 7. Zheng L, T'Kind R, Decuypere S, von Freyend SJ, Coombs GH, Watson DG. 2010. Profiling of
400 lipids in *Leishmania donovani* using hydrophilic interaction chromatography in combination
401 with Fourier transform mass spectrometry. *Rapid Commun Mass Spectrom* 24:2074–2082.
- 402 8. Rojo D, Canuto GAB, Castilho-Martins EA, Tavares MFM, Barbas C, López-González Á, Rivas L.
403 2015. A multiplatform metabolomic approach to the basis of antimonial action and resistance
404 in *Leishmania infantum*. *PLoS One* 10:1–20.
- 405 9. Canuto GAB, Castilho-Martins EA, Tavares M, López-González Á, Rivas L, Barbas C. 2012. CE-
406 ESI-MS metabolic fingerprinting of *Leishmania* resistance to antimony treatment.
407 *Electrophoresis* 33:1901–1910.

- 408 10. Castilho-Martins EA, Canuto GAB, Muxel SM, daSilva MFL, Floeter-Winter LM, del Aguila C,
409 López-González Á, Barbas C. 2015. Capillary electrophoresis reveals polyamine metabolism
410 modulation in *Leishmania (Leishmania) amazonensis* wild-type and arginase-knockout
411 mutants under arginine starvation. *Electrophoresis* 36:2314–2323.
- 412 11. Alves-Ferreira EVC, Toledo JS, De Oliveira AHC, Ferreira TR, Ruy PC, Pinzan CF, Santos RF,
413 Boaventura V, Rojo D, López-González A, Rodríguez, Rosa JC, Barbas C, Barral-Netto M, Barral
414 A, Cruz AK. 2015. Differential Gene Expression and Infection Profiles of Cutaneous and
415 Mucosal *Leishmania braziliensis* Isolates from the Same Patient. *PLoS Negl Trop Dis* 9:1–19.
- 416 12. Scheltema R a, Decuyper S, T'Kindt R, Dujardin J-C, Coombs GH, Breitling R. 2010. The
417 potential of metabolomics for *Leishmania* research in the post-genomics era. *Parasitology*
418 137:1291–1302.
- 419 13. T'Kindt R, Scheltema RA, Jankevics A, Brunker K, Rijal S, Dujardin JC, Breitling R, Watson DG,
420 Coombs GH, Decuyper S. 2010. Metabolomics to unveil and understand phenotypic diversity
421 between pathogen populations. *PLoS Negl Trop Dis* 4.
- 422 14. Saunders EC, Ng WW, Kloehn J, Chambers JM, Ng M, McConville MJ. 2014. Induction of a
423 Stringent Metabolic Response in Intracellular Stages of *Leishmania mexicana* Leads to
424 Increased Dependence on Mitochondrial Metabolism. *PLoS Pathog* 10.
- 425 15. Moreira W, Leprohon P, Ouellette M. 2011. Tolerance to drug-induced cell death favours the
426 acquisition of multidrug resistance in *Leishmania*. *Cell Death Dis* 2:e201.
- 427 16. Paris C, Loiseau PM, Bories C, Bréard J. 2004. Miltefosine Induces Apoptosis-Like Death in
428 *Leishmania donovani* Promastigotes. *Antimicrob Agents Chemother* 48:852–859.
- 429 17. Inbar E, Canepa GE, Carrillo C, Glaser F, Grotemeyer MS, Rentsch D, Zilberstein D, Pereira CA.
430 2012. Lysine transporters in human trypanosomatid pathogens. *Amino Acids* 42:347–360.

- 431 18. Darlyuk I, Goldman A, Roberts SC, Ullmarr B, Rentsch D, Zilberstein D. 2009. Arginine
432 homeostasis and transport in the human pathogen *Leishmania donovani*. *J Biol Chem*
433 284:19800–19807.
- 434 19. Pérez-Victoria FJ, Sánchez-Cañete MP, Castanys S, Gamarro F. 2006. Phospholipid
435 translocation and miltefosine potency require both *L. donovani* miltefosine transporter and
436 the new protein LdRos3 in *Leishmania* parasites. *J Biol Chem* 281:23766–23775.
- 437 20. Gazanion É, Fernández-Prada C, Papadopoulou B, Leprohon P, Ouellette M. 2016. Cos-Seq for
438 high-throughput identification of drug target and resistance mechanisms in the protozoan
439 parasite *Leishmania*. *Proc Natl Acad Sci* 201520693.
- 440 21. Zufferey R, Mamoun C Ben. 2002. Choline transport in *Leishmania major* promastigotes and
441 its inhibition by choline and phosphocholine analogs. *Mol Biochem Parasitol* 125:127–134.
- 442 22. Rakotomanga M, Blanc S, Gaudin K, Chaminade P, Loiseau PM. 2007. Miltefosine affects lipid
443 metabolism in *Leishmania donovani* promastigotes. *Antimicrob Agents Chemother* 51:1425–
444 1430.
- 445 23. Rakotomanga M, Loiseau PM, Saint-Pierre-Chazalet M. 2004. Hexadecylphosphocholine
446 interaction with lipid monolayers. *Biochim Biophys Acta - Biomembr* 1661:212–218.
- 447 24. Lux H, Heise N, Klenner T, Hart D, Opperdoes FR. 2000. Ether-lipid (alkyl-phospholipid)
448 metabolism and the mechanism of action of ether-lipid analogues in *Leishmania*. *Mol*
449 *Biochem Parasitol* 111:1–14.
- 450 25. Wassef MK, Fioretti TB, Dwyer DM. 1985. Lipid analyses of isolated surface membranes of
451 *Leishmania Donovanii* promastigotes. *Lipids* 20:108–115.
- 452 26. Yao C, Wilson ME. 2016. Dynamics of sterol synthesis during development of *Leishmania* spp.
453 parasites to their virulent form. *Parasites & vectors* 9:200.

- 454 27. Denny PW, Smith DF. 2004. Rafts and sphingolipid biosynthesis in the kinetoplastid parasitic
455 protozoa. *Mol Microbiol* 53:725–733.
- 456 28. Zhang K, Pompey JM, Hsu F-F, Key P, Bandhuvula P, Saba JD, Turk J, Beverley SM. 2007.
457 Redirection of sphingolipid metabolism toward de novo synthesis of ethanolamine in
458 *Leishmania*. *EMBO J* 26:1094–104.
- 459 29. Zhang K, Beverley SM. 2010. Phospholipid and sphingolipid metabolism in *Leishmania*. *Mol*
460 *Biochem Parasitol* 170:55.
- 461 30. Ivens AC, Peacock CS, Worthey EA, Murphy L, Berriman M, Sisk E, Rajandream M, Adlem E,
462 Anupama A, Apostolou Z, Attipoe P, Bason N, Beck A, Beverley SM, Bianchetti G, Borzym K,
463 Bothe G, Bruschi C V, Collins M, Cadag E, Ciarloni L, Clayton C, Coulson RMR, Cronin A, Cruz
464 AK, Robert M, Gaudenzi J De, Dobson DE, Duesterhoeft A, Fosker N, Frasch AC, Fraser A,
465 Fuchs M, Goble A, Goffeau A, Harris D, Hertz-fowler C, Horn D, Huang Y, Klages S, Knights A,
466 Kube M, Matthews K, Michaeli S, Mottram JC, Müller- S, Munden H, Nelson S, Norbertczak H,
467 Oliver K, Neil SO, Pentony M, Pohl TM, Price C, Purnelle B, Quail MA, Rabbinowitsch E,
468 Reinhardt R, Rieger M, Rinta J, Robben J, Robertson L, Ruiz JC, Rutter S, Saunders D, Schäfer
469 M, Schein J, Schwartz DC, Seeger K, Seyler A, Sharp S, Shin H, Sivam D, Squares R, Squares S,
470 Tosato V. 2006. NIH Public Access 309:436–442.
- 471 31. Denny PW, Goulding D, Ferguson MAJ, Smith DF. 2004. Sphingolipid-free *Leishmania* are
472 defective in membrane trafficking, differentiation and infectivity. *Mol Microbiol* 52:313–327.
- 473 32. Fridberg A, Olson CL, Nakayasu ES, Tyler KM, Almeida IC, Engman DM. 2008. Sphingolipid
474 synthesis is necessary for kinetoplast segregation and cytokinesis in *Trypanosoma brucei*. *J*
475 *Cell Sci* 121:522–535.
- 476 33. Escobar P, Matu S, Marques C, Croft SL. 2002. Sensitivities of *Leishmania* species to
477 hexadecylphosphocholine (miltefosine), ET-18-OCH₃ (edelfosine) and amphotericin B. *Acta*

- 478 Trop 81:151–157.
- 479 34. Goldman-Pinkovich A, Balno C, Strasser R, Zeituni-Molad M, Bendelak K, Rentsch D, Ephros
480 M, Wiese M, Jardim A, Myler PJ, Zilberstein D. 2016. An Arginine Deprivation Response
481 Pathway Is Induced in *Leishmania* during Macrophage Invasion. *PLoS Pathog* 12:1–18.
- 482 35. Castilho-Martins EA, da Silva MFL, dos Santos MG, Muxel SM, Floeter-Winter LM. 2011.
483 Axenic *leishmania amazonensis* promastigotes sense both the external and internal arginine
484 pool distinctly regulating the two transporter-coding genes. *PLoS One* 6.
- 485 36. Westrop GD, Williams RAM, Wang L, Zhang T, Watson DG, Silva AM, Coombs GH. 2015.
486 Metabolomic analyses of *Leishmania* reveal multiple species differences and large differences
487 in Amino Acid Metabolism. *PLoS One* 10.
- 488 37. Silva AM, Cordeiro-da-Silva A, Coombs GH. 2011. Metabolic variation during development in
489 culture of *leishmania donovani* promastigotes. *PLoS Negl Trop Dis* 5.
- 490 38. Shaw CD, Lonchamp J, Downing T, Imamura H, Freeman TM, Cotton JA, Sanders M, Blackburn
491 G, Dujardin JC, Rijal S, Khanal B, Illingworth CJR, Coombs GH, Carter KC. 2016. In vitro
492 selection of miltefosine resistance in promastigotes of *Leishmania donovani* from Nepal:
493 Genomic and metabolomic characterization. *Mol Microbiol* 99:1134–1148.
- 494 39. Imbert L, Ramos RG, Libong D, Abreu S, Loiseau PM, Chaminade P. 2012. Identification of
495 phospholipid species affected by miltefosine action in *Leishmania donovani* cultures using LC-
496 ELSD, LC-ESI/MS, and multivariate data analysis. *Anal Bioanal Chem* 402:1169–1182.
- 497 40. Zhang O, Wilson MC, Xu W, Hsu FF, Turk J, Kuhlmann FM, Wang Y, Soong L, Key P, Beverley
498 SM, Zhang K. 2009. Degradation of host sphingomyelin is essential for *Leishmania* virulence.
499 *PLoS Pathog* 5.
- 500 41. Fernandez-Prada C, Vincent IM, Brotherton M-C, Roberts M, Roy G, Rivas L, Leprohon P,

- 501 Smith TK, Ouellette M. 2016. Different Mutations in a P-type ATPase Transporter in
502 Leishmania Parasites are Associated with Cross-resistance to Two Leading Drugs by Distinct
503 Mechanisms. *PLoS Negl Trop Dis* 10:e0005171.
- 504 42. Saint-Pierre-Chazalet M, Ben Brahim M, Le Moyec L, Bories C, Rakotomanga M, Loiseau PM.
505 2009. Membrane sterol depletion impairs miltefosine action in wild-type and miltefosine-
506 resistant *Leishmania donovani* promastigotes. *J Antimicrob Chemother* 64:993–1001.
- 507 43. Henke J, Engelmann J, Flogel U, Pfeuffer J, Kutscher B, Nossner G, Engel J, Voegeli R, Leibfritz
508 D. 1998. Apoptotic effects of hexadecylphosphocholine on resistant and nonresistant cells
509 monitored by NMR spectroscopy. *Drugs of Today* 34:37–50.
- 510 44. Ruiter GA, Verheij M, Zerp SF, Van Blitterswijk WJ. 2001. Alkyl-lysophospholipids as
511 anticancer agents and enhancers of radiation-induced apoptosis. *Int J Radiat Oncol Biol Phys*
512 49:415–419.
- 513 45. Rybczynska M, Spitaler M, Knebel NG, Boeck G, Grunicke H, Hofmann J. 2001. Effects of
514 miltefosine on various biochemical parameters in a panel of tumor cell lines with different
515 sensitivities. *Biochem Pharmacol* 62:765–772.
- 516 46. Proto WR, Coombs GH, Mottram JC. 2012. Cell death in parasitic protozoa: regulated or
517 incidental? *Nat Rev Microbiol* 11:58–66.
- 518 47. Dwyer DM. 1976. Antibody-Induced Modulation of *Leishmania Donovanii* Surface Membrane
519 Antigens Information about subscribing to The Journal of Immunology is online at : Antibody-
520 Induced Modulation of *Leishmania donovani* Surface Membrane Antigens. *J Immunol*
521 117:2081–2091.
- 522 48. De Rycker M, Hallyburton I, Thomas J, Campbell L, Wyllie S, Joshi D, Cameron S, Gilbert IH,
523 Wyatt PG, Frearson JA, Fairlamb AH, Gray DW. 2013. Comparison of a high-throughput high-

- 524 content intracellular *Leishmania donovani* assay with an axenic amastigote assay. *Antimicrob*
525 *Agents Chemother* 57:2913–2922.
- 526 49. Godzien J, Ciborowski M, Armitage EG, Jorge I, Camafeita E, Burillo E, Martin-Ventura JL,
527 Rupérez FJ, Vázquez J, Barbas C. 2016. A single in-vial dual extraction strategy for the
528 simultaneous lipidomics and proteomics analysis of HDL and LDL fractions. *J Proteome Res*
529 15:1762–1775.
- 530 50. Godzien J, Armitage EG, Angulo S, Martinez-Alcazar MP, Alonso-Herranz V, Otero A, Lopez-
531 Gonzalez A, Barbas C. 2015. In-source fragmentation and correlation analysis as tools for
532 metabolite identification exemplified with CE-TOF untargeted metabolomics. *Electrophoresis*
533 36:2188–2195.
- 534 51. Godzien J, Alonso-Herranz V, Barbas C, Armitage EG. 2014. Controlling the quality of
535 metabolomics data: new strategies to get the best out of the QC sample. *Metabolomics*
536 11:518–528.
- 537
- 538

539 Table 1: Metabolites identified in *Leishmania donovani* axenic amastigotes and significantly affected by miltefosine.

540

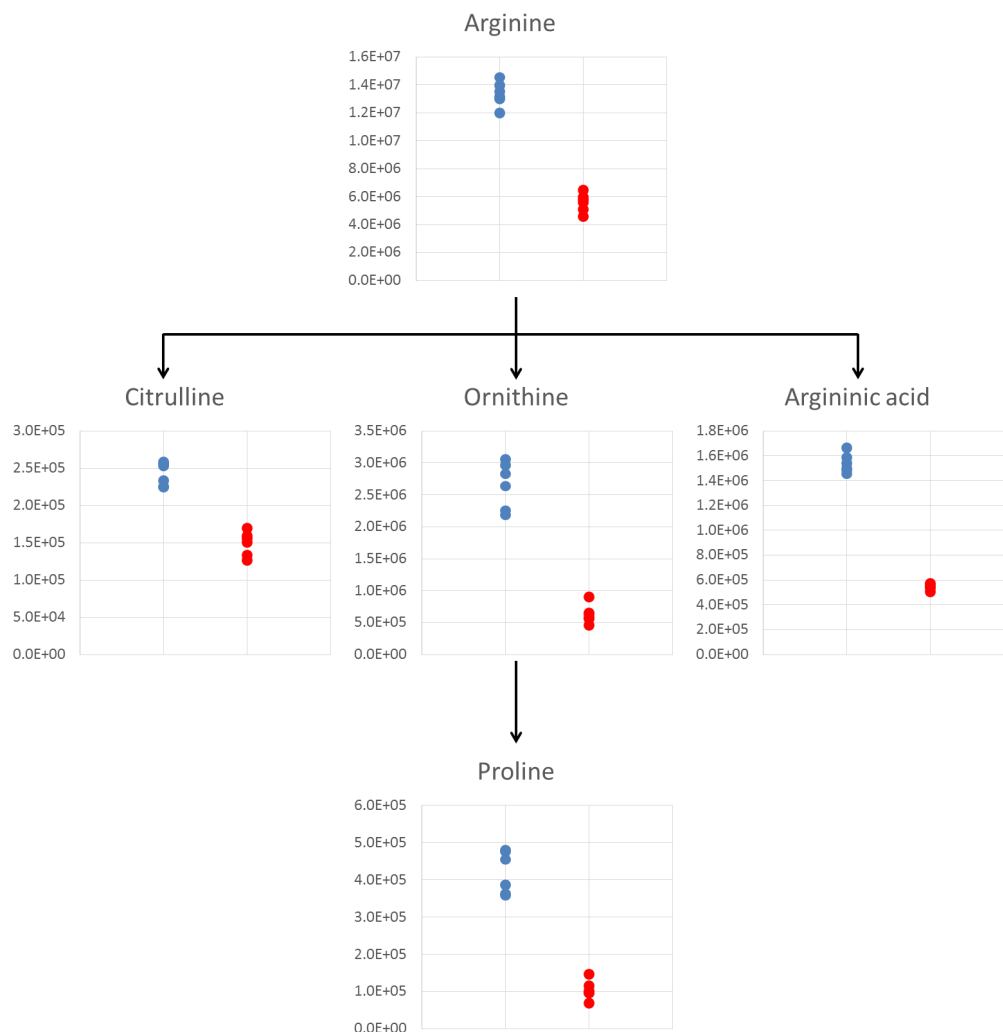
Identification (MSI level 1)	m/z	Migration Time	5 hours				24 hours			
			t-test		Fold change		t-test		Fold change	
			LD	HD	LD	HD	LD	HD	LD	HD
Acetyl-carnitine	204.1232	13.93	3.71E-02	2.30E-05	1.1	1.5	1.28E-03	4.37E-04	1.5	2.4
Adenosine	268.1042	15.23	NS	NS			8.03E-04	4.22E-04	3.7	57.3
Alanine	90.0552	13.95	6.86E-03	2.47E-03	1.3	1.4	2.49E-05	1.33E-06	1.7	5.4
Argininic acid	176.1032	14.19	1.32E-02	2.57E-04	1.2	1.6	9.30E-08	2.85E-08	2.8	6.8
Asparagine	133.0612	15.89	9.15E-03	2.60E-02	1.4	1.3	NS	4.30E-02		1.7
Betaine	118.0862	17.09	1.49E-02	NS	1.2		NS	4.51E-03		1.2
Choline	104.1072	10.92	1.35E-05	NS	1.5		3.24E-04	NS	1.4	
Citrulline	176.1032	16.68	9.08E-03	NS	1.3		1.47E-06	1.39E-05	1.6	1.4
Isoleucine	132.1022	15.52	2.56E-02	1.83E-04	1.3	3.0	1.39E-06	6.56E-06	2.1	4.2
Leucine	132.1022	15.65	4.61E-02	5.08E-03	1.3	1.8	3.91E-03	4.15E-04	1.9	3.2
Lysine	147.1122	11.14	5.50E-04	5.73E-05	1.6	2.7	1.29E-05	1.24E-06	2.1	2.9
Pipecolic acid	130.0862	15.62	6.08E-04	5.05E-04	1.8	1.8	3.78E-03	9.20E-07	1.3	4.3
Valine	118.0862	15.28	2.95E-03	5.84E-06	1.3	2.5	4.36E-06	3.20E-07	2.1	3.6
Glutamic acid	148.0682	16.51	NS	3.22E-05	1.1	1.3	4.18E-04	2.46E-09	1.2	4.7
Aspartic acid	134.0452	17.27	NS	NS			6.56E-03	1.64E-07	1.2	3.0
Creatine	132.0772	13.79	NS	NS			2.42E-04	1.21E-04	1.9	2.5
Histidine	156.0772	11.72	NS	2.49E-03		1.8	1.85E-06	1.55E-06	2.3	11.0
Arginine	175.1192	11.44	NS	9.87E-03		1.3	2.10E-08	1.18E-09	2.4	6.0
Proline	116.0702	11.04	NS	1.39E-02		2.1	5.35E-06	6.07E-06	4.0	40.2
Ornithine	133.0972	11.06	NS	1.45E-02		2.0	7.53E-06	7.94E-06	4.2	34.6
Adenine	136.0612	12.12	NS	NS			4.06E-03	1.90E-03	4.1	17.5
Thiamine	265.1122	10.67	NS	2.19E-02		1.6	1.13E-02	3.73E-02	2.0	2.0
Methionine	150.0592	16.17	NS	NS			4.43E-05	7.76E-05	2.2	6.4
S-adenosylhomocysteine	385.1292	13.73	NS	3.87E-02		1.5	2.68E-03	7.44E-05	1.8	NC
Trans-4-Hydroxyproline	132.0652	17.99	NS	NS			1.09E-05	1.25E-05	1.3	1.4
Phenylalanine	166.0872	16.65	NS	NS			6.82E-03	8.71E-03	1.4	2.0
Carnitine	162.1122	13.30	NS	2.15E-03		1.2	9.26E-08	1.93E-08	1.5	3.7

541

542 Metabolites identified in CE-MS analysis of *Leishmania donovani* axenic amastigotes as being significantly
543 affected by miltefosine treatment in different doses/time-points. All identifications have been determined
544 at MSI level 1, as defined by the analysis of authentic standards. Calculated *p*-values (Student's two-tailed *t*-
545 test (*n*=6 per group) and fold changes are shown for the lower dose (LD: 4.47 μM) or higher dose (HD: 13.41
546 μM) versus the un-treated samples at the respective time-point. Where *p*-values were not significant (NS: *p*

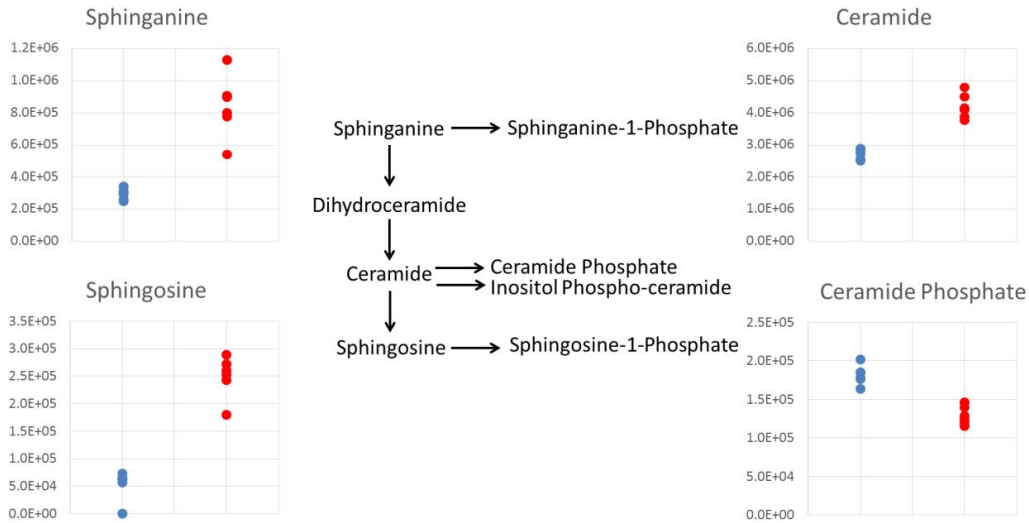
547 > 0.05), there were no fold changes to report. Fold changes are absolute; all are decreases except those
 548 highlighted in grey which are calculated increases with miltefosine with respect to un-treated controls.

549 **Figures**

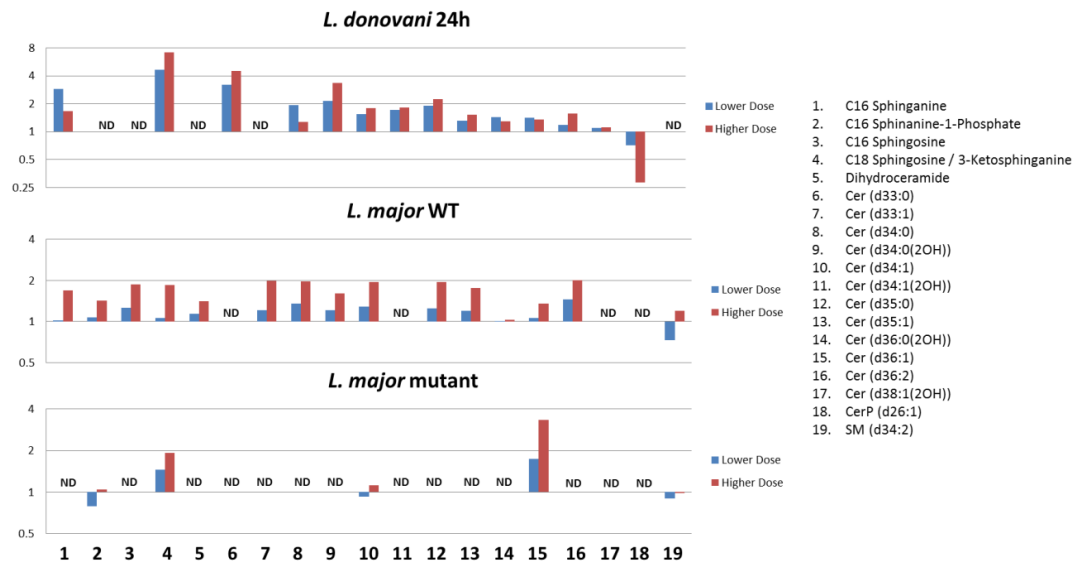


550

551 **Figure 1: Effect of miltefosine on arginine metabolism observed in *L. donovani* axenic amastigotes after 24h**
 552 **of exposure at the lower dose of 4.47 μM . Plots show peak area abundances detected in samples: un-**
 553 **treated parasites in blue, parasites treated with 4.47 μM miltefosine in red.**

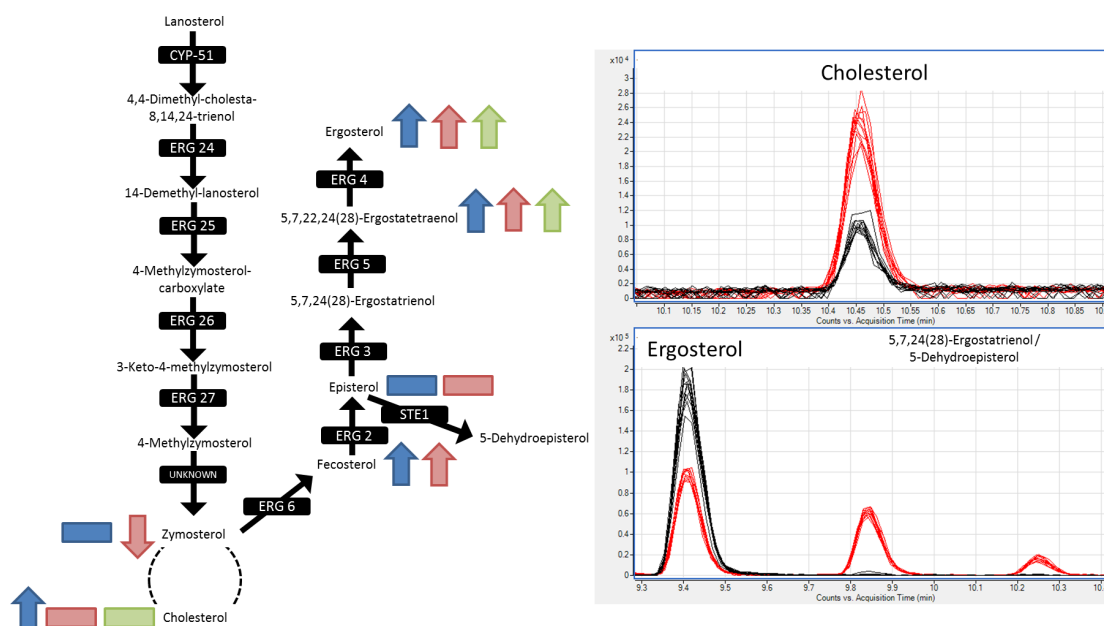


554
 555 **Figure 2: Effect of miltefosine on the SL biosynthetic pathway observed in *L. donovani* axenic amastigotes**
 556 **after 24h of exposure at the lower dose of 4.47 μ M. Plots show peak area abundances for key SLs detected**
 557 **in samples: un-treated parasites in blue, parasites treated with 4.47 μ M miltefosine in red. Sphinganine**
 558 **shown is C16 form, Ceramide shown is 34:1 form, Sphingosine shown is 18:1 form and ceramide phosphate**
 559 **shown is 26:1 form. Plots show trends representative of all detected SLs of their type. For full list of detected**
 560 **SLs, refer to Supplementary Table 3.**



561
 562 **Figure 3: Fold changes in abundance of all SLs detected in *L. donovani* axenic amastigotes and / or *L. major***
 563 **promastigotes, comparing treated parasites to un-treated parasites. Lower dose and higher dose data are**

564 shown for each, corresponding to 4.47 μM and 13.41 μM respectively for *L. donovani* and 10 μM and 30 μM
 565 respectively for *L. major*. SLs that were not detected in a certain dataset are marked with 'ND', while X
 566 denotes complete absence in drug treated parasites and presence in un-treated parasites.



567
 568 **Figure 4: Ergosterol biosynthesis pathway. Sterols increased, decreased or detected but with no change as a**
 569 **response to miltefosine exposure are shown on the pathway (*L. donovani* axenic amastigotes with 5h drug**
 570 **exposure in blue; *L. donovani* axenic amastigotes with 24h drug exposure in red; *L. major* wild type**
 571 **promastigotes in green). In all cases, trends were seen for both low and high concentrations of miltefosine**
 572 **treatment. Chromatographic peaks shown for ergosterol, cholesterol, 5,7,24(28)-Ergostatrienol and 5-**
 573 **dehydroepisterol in *L. major* wildtype (black trace) and ΔLCB2 mutants (red trace) to highlight the**
 574 **differences in sterol profiles between them. 5,7,24(28)-Ergostatrienol and 5-dehydroepisterol share the**
 575 **same logP and therefore it is not possible to distinguish which peak (9.8-9.9 min or 10.2-10.3 min) these**
 576 **sterols correspond to.**

